

A New Manganese Coordination Polymer Based on Azobenzene Tetracarboxylate and Auxiliary Pyridine Ligand: Synthesis, Crystal Structure and Magnetic Property^①

FENG Xun^{a②} SHANG Ya-Pei^c WANG Li-Ya^b

HONG Man-Zhou^c FANG Hai-Peng^a

ZHAO Xin^a LI Zhong-Jun^c

^a (College of Chemistry and Chemical Engineering and Henan Key Laboratory of

Function Oriented Porous Materials, Luoyang Normal University, Luoyang 471934, China)

^b (College of Chemistry and Pharmacy Engineering, Nanyang Normal University, Nanyang 473601, China)

^c (College of Chemistry, Zhengzhou University, Zhengzhou 450001, China)

ABSTRACT A new manganese coordination polymer (CP) has been synthesized under hydrothermal conditions. Its formula is $\{Mn_2(Oaobtc)(bpe)(H_2O)_4\}_n$, where H_4Oobtc represents oxide azobenzene 2,2',3,3'-tetracarboxylic acid, and bpe is 1,2-bis(4-pyridine) ethylene. It was characterized by elemental analysis, infrared spectrum and X-ray single-crystal diffraction. The coordination polymer crystallizes in the monoclinic system, space group $P2_1/c$. The central ion was coordinated with H_4Oobtc ligands using bridging model, and carboxylic group connects two adjacent Mn(II) ions into dimer units. The oxygen from carboxylates connect these dimer units into a one-dimensional (1D) chain, and N atoms from the bpe further expanded them into three-dimensional (3D) supramolecular edifice, eventually. Variable-temperature magnetic measurements of CP **1** indicate the presence of weak antiferromagnetic exchange between two nearest Mn(II) ions with $J = -0.367 \text{ cm}^{-1}$.

Keywords: acetate bridging, manganese(II), X-ray crystal structure, oxidation azoxybenzene-2,2',3,3'-tetracarboxylic acid, antiferromagnetic interaction; DOI: 10.14102/j.cnki.0254-5861.2011-2809

1 INTRODUCTION

Currently, transition metal coordination polymers (CPs) have recently attracted great attention due to their intriguing architectures and potential applications in functional materials^[1, 2]. The realization of compositionally and structurally designed CPs and their functions remains a significant challenge nowadays owing to the difficulty in fine-tuning properties and architectures of the final products. An effective synthetic approach to obtain functional compounds with predictable properties is to choose the candidate metal centers bearing specifying electronic configuration with coordination preferences and organic bridging linkers, even appropriate auxiliary ligands^[3]. Among organic linkers, multicarboxylic

acids can bind several metal centers with appropriate coordination geometry to construct polynuclear clusters or metal organic frameworks. Phenyl or pyridine based aromatic substituted multicarboxylates have been varied to be a functional ligand, which can construct one- to three-dimensional (3D) compounds, with catalysis, electrochemical, magnetism characters, etc^[5-7]. The chemical modified ligands, such as compounds containing an azo ($-N=N-$) group as light-harvesting chromophore, are always employed to enhance/reduce the light adsorption, and then facilitate/delay energy transferring to luminescence centers to achieve efficient emission. Azomethines and azonium pyrrolidine derivative have been employed in light-emitting optical materials^[8], and some of transition/lanthanide metal compounds containing

Received 16 March 2020; accepted 2 July 2020 (CCDC 1984219)

① This project was supported by the National Foundation for Science of China (No. U1804131 and 21671114), and Foundation for Science & Technology Innovation Talents in Henan province (No. 16410010012)

② Corresponding authors. Tel.: +86-379-68618327, E-mails: fengx@lynu.edu.cn and wlya@lynu.edu.cn

this spacer separated aromatic tetracarboxylate have been documented^[9, 10]. On the other hand, bpe, as the N donor rigid ligand, has been proved to be a good candidate used as polymeric linkers for constructing fascinating coordination polymers in the field of potential functional materials^[11]. The coordination of neutral ligands with metal centers can also largely change coordination environments, resulting in the tuning of magnetic property^[12]. Single-molecule magnets (SMMs) containing transition metal have attracted a great deal of attention during the last two decades^[13, 14], because of their potential applications in information processing, quantum computing, high density data storage and molecular spintronics. Moreover, phenoxo functions and carboxylatebridged Mn(II) complexes are well recognized from magnetic point of view as the high-spin Mn(II) ion contains five unpaired electrons, and thus the assembly of Mn(II) with multicarboxylate is inclined to the formation of single-molecule magnets (SMMs)^[15, 16]. Binuclear Mn(II) complexes were treated as models for understanding the effect of structural parameters in determining the sign and magnitude of exchange coupling interactions between neighboring magnetic centers. In order to further study coordination behavior and role of bpe, and to further study the influence of magnetic properties, in this contribution a new manganese compound containing H₄Oaobtc acid and bpe ligand has been obtained and systematically characterized.

2 EXPERIMENTAL

2.1 Materials and physical measurements

All reagents and solvents were of AR grade and used without further purification. Elemental analyses for C, H and N were carried out on an Elementar Vario EL elemental analyzer. Diffraction studies on single crystals were conducted on a Bruker diffractometer applying graphite-monochromated MoK α radiation ($\lambda = 0.71073$ Å). The infrared spectra (4000~400 cm⁻¹) were recorded by using KBr pellet on an Avatar TM 360 E.S.P. FTIR spectrometer. Thermogravimetry and differential thermal analysis were recorded using a Thermogravimetric analyses (TGA) in nitrogen at a heating rate of 10 °C min⁻¹ using a TG/DTA 6300 integration thermal analyzer. XRPD measurements were carried out at room temperature using a Bruker D8 Advance powder diffractometer with CuK α radiation ($\lambda = 1.5408$ Å) with a scan speed

of 0.2 s per step and a step size of 0.02 (2 θ). The crushed crystalline powder samples were scanned at 40 kV and 40 mA from 5 to 50°. Temperature dependent magnetic susceptibilities were recorded on a MPMS magnetometer from 2 to 300 K with an applied field of 2 kOe. Pascal's constants were used to estimate the correction for the underlying diamagnetism of the sample.

2.2 Synthesis and crystallization of compound

[Mn₂(Oaobtc)(bpe)(H₂O)₄]_n (1)

H₄oobtc acid (0.1 mmol, 0.038 g) and bpe (0.1 mmol, 0.019 g) were mixed and dissolved in 30 mL aqueous solution of water/DMF ($v/v = 2.0$, 12 mL). After that they were mixed with an aqueous solution (10 mL) of Mn(CH₃COO)₂ · 4H₂O (0.049 g, 0.2 mmol). After stirring for 20 min in air, the pH value was adjusted to 6.5 with acetic acid, and the mixture was placed into a 25 mL Teflon-lined autoclave under autogenous pressure being heated at 120 °C for 48 h, then the autoclave was cooled over a period of 24 h at a rate of 5 °C h⁻¹. After filtration, the products were washed with distilled water and dried. The black block-shaped crystals suitable for X-ray diffraction had been obtained. Yield: 36 mg (48% based on manganese element). Elemental analysis for C₁₄H₁₂MnN₂O₇ (calcd. C, 44.81; H, 3.22; N, 7.47%). Found: C, 44.59; H, 3.40; N, 7.39%.

2.3 Single-crystal X-ray structure determination

One crystal with dimensions of 0.22 × 0.18 × 0.15 mm³ was selected for measurement. A total of 6817 reflections were collected at room temperature for the φ - ω scan technique in the range of 3.38° ≤ θ ≤ 26.83°. Structure was solved by direct methods and subsequently completed by Fourier recycling by using the SHELXTL software packages. The obtained models were refined with version 2014 of SHELXL against F^2 on all data by full-matrix least squares^[17, 18]. A full-matrix least-squares refinement on F^2 was carried out using SHELXL-97. The final $R = 0.0444$, $wR = 0.1215$ ($w = 1/[\sigma^2(F_o^2) + (0.0502P)^2 + 4.8549P]$, where $P = (F_o^2 + 2F_c^2)/3$), $S = 1.159$, $F(000) = 2016$, $T = 291(2)$ K, $(\Delta\rho)_{\max} = 0.46$ and $(\Delta\rho)_{\min} = -0.72$ e/Å³. In both systems, all non-hydrogen atoms were refined anisotropically, and the hydrogen atoms were set in calculated positions and refined isotropically by using the riding model. Residual peaks in difference Fourier map could be assigned as positions of hydrogen atoms belonging to water molecules. The selected bond lengths and bond angles are reported in Table 1.

Table 1. Selected Bond Lengths (Å) and Bond Angles (°) for Compound **1**

Bond	Dist.	Bond	Dist.	Bond	Dist.
O(4)–Mn(1 ²)	2.170(2)	Mn(1)–O(3)	2.137(2)	Mn(1)–O(4 ¹)	2.170(2)
Mn(1)–O(5)	2.291(2)	Mn(1)–O(6)	2.161(2)	Mn(1)–N(3)	2.262(2)
Angle	(°)	Angle	(°)	Angle	(°)
O(1)–Mn(1)–O(4 ¹)	90.55(9)	O(1)–Mn(1)–O(5)	172.67(9)	O(1)–Mn(1)–O(6)	100.19(10)
O(1)–Mn(1)–N(3)	93.37(9)	O(3)–Mn(1)–O(1)	85.64(10)	O(3)–Mn(1)–O(4 ¹)	100.58(10)
O(3)–Mn(1)–O(5)	89.70(11)	O(3)–Mn(1)–O(6)	168.42(10)	O(1)–Mn(1)–N(3)	84.42(10)
O(4 ¹)–Mn(1)–O(5)	84.74(9)	O(4 ¹)–Mn(1)–N(3)	173.88(9)	O(6)–Mn(1)–O(4 ¹)	89.43(9)
O(6)–Mn(1)–O(5)	85.40(11)	O(6)–Mn(1)–N(3)	85.25(10)	N(3)–Mn(1)–O(5)	91.80(10)
C(7)–O(1)–Mn(1)	129.28(19)	C8(1)–O(3)–Mn(1)	138.8(2)	C(8)–O(4)–Mn(1 ²)	129.11(19)
C(9)–N(3)–Mn(1)	121.2(2)	C(14)–N(3)–Mn(1)	122.5(2)	N(8)–Mn(1)–O(2)	173.05(10)

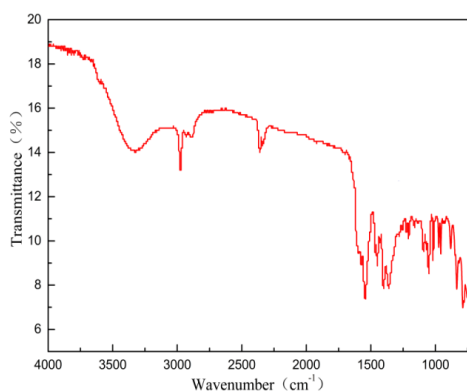
Symmetry codes: (1) $x, 3/2 - y, -1/2 + z$; (2) $x, 3/2 - y, 1/2 + z$

3 RESULTS AND DISCUSSION

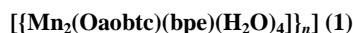
3.1 Infrared spectra of **1**

As illustrated in Fig. 1, in IR spectra of the title compound, the weaker and broad peak in the frequency region of $3450 \sim 3500 \text{ cm}^{-1}$ is attributed to $\text{O} \cdots \text{H}$ bonding stretching vibration of coordination water molecules. The sharp bands in the

ranges of $1600 \sim 1500$ and $1460 \sim 1350 \text{ cm}^{-1}$ are attributed to asymmetric and symmetric stretching vibrations of carboxylic groups from Oaobtc ligand, respectively. No peaks exist at about 1710 cm^{-1} , which indicates the tetracarboxylic acid molecules in this complex have been completely deprotonated. The ligand bpe showed its backbone vibration peaks $\nu_{(\text{C}=\text{N})}$ at 1510 cm^{-1} [19].

**Fig. 1.** Fourier transforms infrared spectrum of coordination polymer **1**

3.2 Structure description for



The perspective view of the molecular structure of coordination polymer **1** is illustrated in Fig. 2. The title compound crystallizes in monoclinic system, space group $P2_1/c$. The asymmetric unit contains one Mn(II) cation, half an oaoctc ligand, half of bpe ligand and two coordinated water molecules. Remarkably, during the hydrothermal condition, H_4aobtc acid has been oxidized into H_4Oaobtc acid possible due to the presence of Mn(II) cation as catalysis[20]. All four carboxylic groups of H_4aobtc acid ligand are deprotonated, and exhibit a bridging ligand linking Mn(II) ions using a monodentate model, rather than chelating coordination fashion as presented in Fig. 2a. It is noted that different acid/base conditions result in discrepancy deprotonation degree in tetracarboxylic groups in ligand, which is beneficial

to modulate the structure[21]. The Mn(II) ion is hexa-coordinated with a pseudo octahedral geometry, bearing a N_1O_5 donor set around it. Among the donor set, the two O atoms coordinated to Mn(II) from terminal H_2O ligand and other two O atoms of carboxylic moieties from Oaobtc are located in equatorial plane. The N atom from bridging bpe and one O atom derived from carboxylic groups of Oaobtc anion ligand are located in axis positions, completing the octahedron coordination geometry. The Mn–O distances range from 2.137(2) to 2.291(2) Å (Table 2 and Fig. 1). In contrast, average Mn–N distance is found to be 2.262(2) Å, consistent with other Mn(II) complexes reported previously[2, 16]. The O–Mn–O angles vary from $85.64(10)$ to $173.05(10)^\circ$, which are comparable to the geometry observed in related Mn(II) complexes[12, 13].

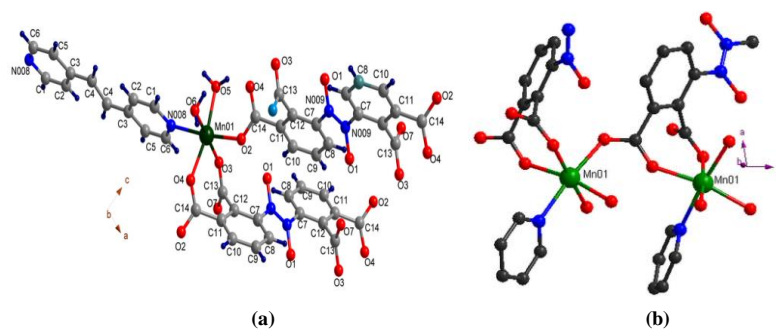


Fig. 2. (a) View of the coordination environment of Mn(II) ion in asymmetric unit of coordination polymer 1. Color codes: dark green, Mn; blue, N; red, O; gray black, C. (b) View of dimer in the asymmetric unit of 1 with some hydrogen atoms omitted for clarity

It is notable that the bond angles of N(8)–Mn(1)–O(2), N(3)–Mn(1)–O(5) and O(1)–Mn(1)–O(5) are 173.05(10), 91.80(10) and 172.67(9)°, which means the Mn(II) ion is located in a slightly distorted octahedron coordination environment. Interestingly, the acetate group from Oaobtc exhibits *u*₂-*cis*, *trans*-bridge modes to connect the two adjacent Mn(II) ions into a binuclear unit with the Mn··Mn distance of 5.374 Å, as displayed in Fig. 1b. The angle for Mn(1)¹–O(6)–Mn(1) is 150.34°, which provides steric relief for the binding of solvent water molecules; it also separates the Mn centers quite far way. These binuclear units are further connected into an infinite 1D zigzag chain approximately along the *ac* plane, as displayed in Fig. 3a. In fact, Oaobtc acts as a terminal ligand rather than exhibits a bridge model connecting dimer units into infinite 1D chains. Moreover, the ancillary ligand bpe molecules act as cross bridging, and link neighboring metal-organic chains into a regular 2D layer with the interchain Mn··Mn separation of 13.862 Å, as displayed in Fig. 3b. In such a manner, a square (4, 4) grid layer with dangling pyridine arms is generated.

This layer skeleton is close to other Mn(II) coordination polymers containing bpe ligand^[12, 16, 21]. In fact, this liner ligand can also exhibit a monodentate linker or non-coordinating modes^[22] due to its various bridging fashions and strong coordination tendency. It is able to generate 1D robust chain, or to be pillar ligand to construct high-dimensional architecture, exhibiting strong luminescence since the ethylene bonds of the dyes are preorganized for stereospecific [2+2] photocycloaddition (PCA) induced by visible light^[22]. The coordination fashion in this case is also found in relevant transition metal compounds based on phthalate and bipyridinyl ligands^[12], but it is essentially different from either relevant silver coordination polymer or dinuclear manganese(III) complexes with pentaanionic pentadentate ligands including alkoxo, amido, and phenoxo donors^[24, 25]. The 2D networks with non-penetrating feather above mentioned are further inter connected into a 3D supramolecular framework edifice through carboxylate and with hydrogen bonding, as shown in Fig. 4.

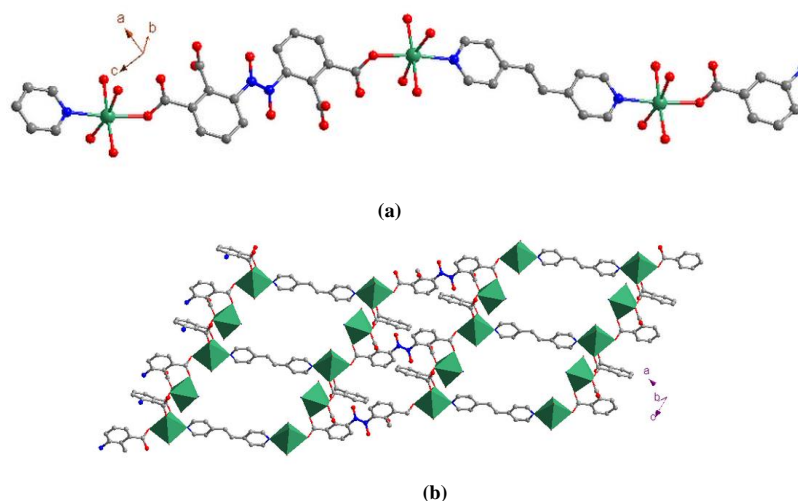


Fig. 3. (a) Perspective view of 1D alternate zigzag chains along the *b* axis. (b) Perspective view of (4, 4) grid layer along the *b* axis in coordination polymer 1

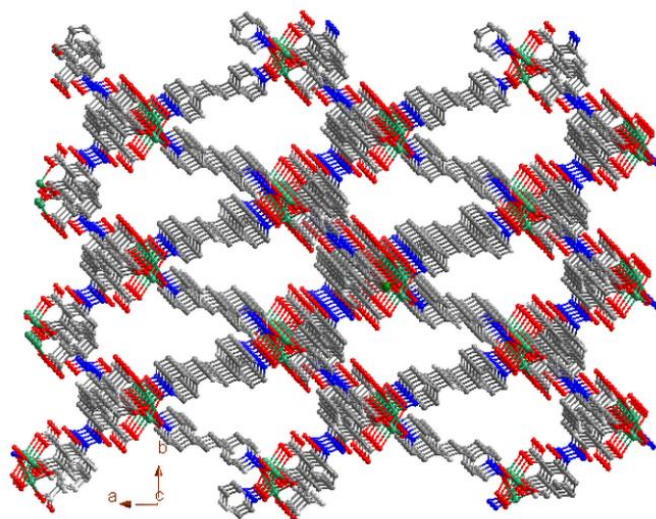


Fig. 4. Projection of the 3D packing crystal structure of **1** along the *c* axis

3.3 X-ray diffraction powder pattern and thermogravimetry analysis

To verify the phase purity of coordination polymer **1**, the bulk sample was characterized by PXRD at room temperature. As depicted in Fig. 5a, the peak positions of the experimental patterns for compound **1** (final bulk material) are nearly identical to the correspondingly simulated ones generated from single-crystal X-ray diffraction data, although some minor Bragg peak positions have been shifted in comparison to the simulated ones due to discrepancy between powder and crystalline materials. The TGA experiment was performed

under N₂ atmosphere at a heating rate of 10 °C min⁻¹ in the temperature range of 20~900 °C. As reported in Fig. 5b, the initial weight loss process takes place at about 150 °C, corresponding to release of two water molecules (calcd. 9.58%). Subsequently, upon further heating it till beyond 200 °C, compound **1** decomposes and significant weight loss of 35.23% is found in a temperature range of 260~400 °C, which corresponds to destruction of one Oaobtc ligand (calcd. 51.2%). As the temperature is increased beyond 600 °C, the further weight loss till 900 °C may be roughly in accordance to the release of bpe ligand.

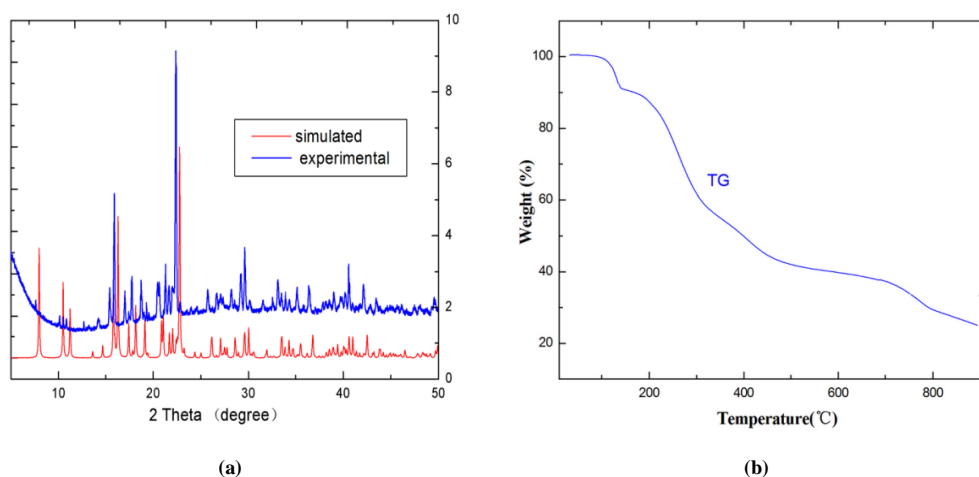


Fig. 5. (a) Comparison of stimulated (blue) and experimental (red) powder XRD patterns of coordination polymer **1**. (b) Thermogravimetric curves for coordination polymer **1**

3.4 Magnetic property

The plot of $\chi_M T$ and χ_M vs. *T* susceptibility for coordination polymer **1** is presented in Fig. 6. The value of $\chi_M T$ at 300 K

amounts to 8.83 cm³·mol⁻¹ K, which is slightly higher than the expected spin-only value for two high-spin Mn(II) ions (8.75 cm³·mol⁻¹·K)^[26]. As the temperature is lowered, the $\chi_M T$

value is almost constant in region of 150~300 K and then rapidly decreases to $1.32 \text{ cm}^3 \cdot \text{mol}^{-1} \cdot \text{K}$ at 1.9 K, indicating the presence of possible antiferromagnetic interactions within the coordination polymer. According to the structure analysis mentioned above, the intramolecular $\text{Mn}^{\text{II}} \cdots \text{Mn}^{\text{II}}$ separation is 13.08 Å, while the shortest intermolecular $\text{Mn}^{\text{II}} \cdots \text{Mn}^{\text{II}}$ distance is 5.374 Å. It could be presumed that the main magnetic interactions between two Mn^{II} centers should happen within 1D chain through acetate bridging. Meanwhile, considering the magnetic interaction between manganese pairs within these 1D zigzag chains, two coupling parameters J and zJ' may be considered to interpret two possible magnetic interactions in **1**. Here, J is the exchange coupling parameter between adjacent $\text{Mn}^{\text{II}}\text{-Mn}^{\text{II}}$ within dimer and zJ' accounts for interactions between the chains. The magnetic data were thus approximately analyzed by an isotropic Heisenberg model for the uniform chains generated by Hiller *et al.*^[27], for high spin $S = 5/2$. In order to quantitatively understand the magnitude of the spin-exchange interaction,

the following Eq. (1) is induced from the spin Hamiltonian $\hat{H} = -J\hat{S}_1\hat{S}_2$ to evaluate exchange-coupled high-spin dinuclear $\text{Mn}(\text{II})$ complex^[4, 12, 28].

$$\hat{H} = -J\hat{S}_1\hat{S}_2 \dots\dots\dots (1)$$

$$\chi_{Mm2} = \frac{Ng^2\beta^2}{4KT} \left[\frac{A}{B} \right] \dots\dots\dots (2)$$

$$A = 8(e^x + 5e^{3x} + 14e^{6x} + 30e^{10x} + 55e^{15x})$$

$$B = (1 + 3e^x + 5e^{3x} + 7e^{6x} + 9e^{10x} + 11e^{15x})$$

Where $x = |J|/KT$. An additional coupling parameter, zJ' , was added in Eq. (2) to take into account the magnetic behavior between the 1-D chains as a molecular field approximation^[29] to explain the actual magnetic property of **1**.

$$\chi_M = \frac{\chi_{bi}}{1 - \frac{2zJ'}{N\beta^2g^2} \chi_{bi}} \dots\dots\dots (3)$$

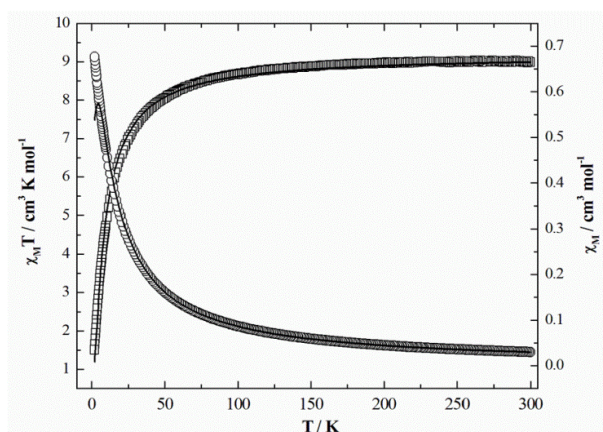


Fig. 6. Temperature dependence of $\chi_M T(\square)$ and $\chi_M(\circ)$ versus T for coordination polymer **1**.
The solid line represents the best fit obtained from the Hamiltonian given in the text

The least-squares fitting of magnetic susceptibilities leads to $J = -0.367$, $g = 2.02$, $zJ' = -0.22 \text{ cm}^{-1}$, and $R = 1.16 \times 10^{-3}$ ($R = \Sigma[(\chi_M)_{\text{obs}} - (\chi_M)_{\text{calc}}]^2 / \Sigma[(\chi_M)_{\text{obs}}]^2$). The small negative values of J and zJ' further corroborate the presence of weak antiferromagnetic interactions between $\text{Mn}(\text{II})$ ions and the interactions between 1D chains. It is interesting to compare the magnetic properties with analogous complexes containing Mn clusters previously reported. For example, isophthalato bridged trimanganese clusters, $\{[\text{Mn}_3(\text{H}_2\text{O})_2(\text{H-bpp})_2(5\text{-brip})_4] \text{bpp} = 1,3\text{-bi}(4\text{-pyridyl}) \text{ propane, which contains 4,5-bromoisophthalic acid and bpe } (J = -1.67 \text{ cm}^{-1}, g = 2.00)^{[30]}$. The coupling interaction in this case is weaker than that of tetranuclear cluster, $[\text{Mn}_4(\text{tbip})_4(\text{bbp})_2(\text{H}_2\text{O})_2]$ ($J =$

-0.49 cm^{-1} , $g = 2.26$, $\text{H}_2\text{tbip} = 5\text{-tert-butyl-isophthalic acid, bbp} = 1,3\text{-bis}(\text{benzimidazol})\text{propane}$); and $[\text{C}(\text{NH}_2)_3]_8[\text{Mn}^{\text{II}}]_4\text{-(cit)}_4] \cdot 8\text{H}_2\text{O}$ ($J = -0.82 \text{ cm}^{-1}$, $g = 1.92$, $\text{cit} = \text{citrate}$)^[31]. It is found that a moderate strong antiferromagnetic coupling interaction was mediated through the methanolato oxygen bridge between two $\text{Mn}(\text{III})$ ions and the exchange parameter. It gives result as $J = -3.6 \text{ cm}^{-1}$ ^[32]. The domain antiferromagnetic interactions obtained for the title compound are also comparable to 1D chain $\text{Mn}(\text{II})$ coordination polymers containing 2,2':6',2''-terpyridine-4'-carboxylic acid and 4'-(4-carboxyphenyl)-2,2':6',2''-terpyridine^[4], in which the best fitting parameters are $J = -0.88 \text{ cm}^3 \text{ K mol}^{-1}$ and $g = 2.046$. It is also weaker than that of oxalate bridged Mn

binuclear complex containing N_3O -donor chelate ligand, $[\{(\text{bpppa})\text{Mn}\}_2(\mu\text{-C}_2\text{O}_4)](\text{ClO}_4)_2$ with $J = -2.95 \text{ cm}^{-1}$, $g = 2.0$ and $zJ \approx 0 \text{ cm}^{-1}$ [33].

4 CONCLUSION

In summary, we have presented a new manganese coordination polymer constructed by azoxybenzenetetracarboxylic acid along with linear bpe ligand. The auxiliary

N-donor ligands, coordination modes of metal ions and configurations of multicarboxylate ligands play synergistic roles in governing the final coordination polymer edifice. The magnetic properties study indicate the existence of moderate intramolecular antiferromagnetic couplings. This work not only enriches the coordination chemistry of later transition metal cation, but also maybe provides a useful reference for the design and synthesis of other discrete magnetic materials base on aromatic polycarboxylic acid ligands.

REFERENCES

- (1) Tang, L.; Shi, D. Q.; Wang, Y. L.; Yin, S. Y.; Wang, J. J.; Hou, X. Y. Structures and properties of two pillared-layer Mn(II) MOFs with 5-ethyl-pyridine-2,3-dicarboxylate. *Chin. J. Struct. Chem.* **2019**, 38, 1600–1608.
- (2) Yu, Y. Z.; Chang, S. Y.; Han, X.; Chen, G. X.; Xuan, Y. W.; Wu, X. L.; Wang, F. Hydrothermal synthesis, crystal structure and luminescence property of a 2D manganese(II) coordination polymer. *Chin. J. Struct. Chem.* **2019**, 38, 147–154.
- (3) Du, Z. Y.; Prosvirin, A. V.; Mao, J. G. Novel manganese(II) sulfonate-phosphonates with dinuclear, tetranuclear, and hexanuclear clusters. *Inorg. Chem.* **2007**, 46, 9884–9894.
- (4) Zhang, M. B.; Zhang, N.; Hu, R. X. Single and double chainlike manganese coordination polymers of linear ligands: synthesis, structure and magnetism. *Chin. J. Struct. Chem.* **2019**, 38, 301–307.
- (5) Liu, Q.; Yu, L. L.; Wang, Y. Y.; Ji, Z.; Horvat, J.; Cheng, M. L.; Jia, X. Y.; Wang, G. X. Manganese-based layered coordination polymer: synthesis, structural characterization, magnetic property, and electrochemical performance in lithium-ion batteries. *Inorg. Chem.* **2013**, 52, 6, 2817–2822.
- (6) Feng, X.; Xu, C.; Wang, Z. Q.; Tang, S. F.; Fu, W. J.; Ji, B. M.; Wang, L. Y. Aerobic oxidation of alcohols and the synthesis of benzoxazoles 2-catalyzed by a cuprocupric coordination polymer (Cu+–CP) assisted by TEMPO. *Inorg. Chem.* **2015**, 54, 2088–2090.
- (7) Feng, X.; Tian, A. Q.; Li, T. F.; Wang, L. Y.; Lei, P. P. Hydrothermal synthesis, crystal structure and characterization of a 1D neodymium(III) coordination polymer containing the pyridine 2,6-dicarboxylate and oxalate ligands. *Russ. J. Coord. Chem.* **2011**, 37, 823–828.
- (8) Dong, M.; Babalhavaeji, A.; Collins, C. V.; Jarrah, K.; Sadovski, O.; Dai, Q.; Woolley, G. A. Near-infrared photoswitching of azobenzenes under physiological conditions. *J. Am. Chem. Soc.* **2017**, 139, 13483–13486.
- (9) Arıcı, M.; Yeşilel, O. Z.; Taş, M. Coordination polymers assembled from 3,3',5,5'-azobenzenetetracarboxylic acid and different bis(imidazole) ligands with varying flexibility. *Cryst. Growth Des.* **2015**, 15, 3024–3031.
- (10) Feng, X.; Chen, H. P.; Li, R. F.; Yang, M. T.; Guo, S. L.; Wang, L. Y.; Liang, Q. R.; Li, Z. J. Cationic bipy induced the three dimensional supramolecules based on azoxybenzene tetracarboxylate: structures and NIR luminescence property. *Polyhedron* **2019**, 157, 420–427.
- (11) Kitagawa, S.; Kitaura, R.; Noro, S. Functional porous coordination polymers. *Angew. Chem. Int. Ed.* **2004**, 43, 2334–2375.
- (12) Feng, X.; Liu, J.; Li, J.; Ma, L. F.; Wang, L. Y.; Ng, S. W.; Qin, G. Z. J. Series of coordination-polymers based on 4-(5-sulfo-quinolin-8-yloxy) phthalate and bipyridinyl coligands: structure diversity and properties. *Solid State Chem.* **2015**, 80, 230–236.
- (13) Gomez, V.; Corbella, M.; Aullon, G. Two temperature-independent spinomers of the dinuclear Mn(III) compound $[\{\text{Mn}(\text{H}_2\text{O})(\text{phen})\}_2(\mu\text{-2-ClC}_6\text{H}_4\text{COO})_2(\mu\text{-O})](\text{ClO}_4)_2$. *Inorg. Chem.* **2010**, 49, 1471–1480.
- (14) Feng, X.; Ling, X. L.; Liu, L.; Wang, Y. A series of 3D lanthanide frameworks constructed from aromatic multi-carboxylate ligand: structural diversity, luminescence and magnetic properties. *Dalton Trans.* **2013**, 42, 10292–10303.
- (15) Costes, J. P.; Dahan, F.; Donnadiou, B.; Rodriguez Douthon, M. J.; Boussekou, A.; Tuchagues, J. P. Synthesis, structures, and magnetic properties of novel mononuclear, tetranuclear, and 1D chain Mn(III) complexes involving three related asymmetrical trianionic ligands. *Inorg. Chem.* **2004**, 43, 2736–2744.
- (16) Tsai, H. L.; Yang, C. I.; Wernsdorfer, W.; Huang, S. H.; Jhan, S. Y.; Liu, M. H.; Lee, G. H. Mn(II) single-molecule-magnet-based polymers of a one-dimensional helical chain and a three-dimensional network: syntheses, crystal structures, and magnetic properties. *Inorg. Chem.* **2012**, 51, 13171–13180.
- (17) Sheldrick, G. M. *SHELXL-2014/7, Program for the Solution of Crystal Structure*. University of Göttingen, Germany **2014**.
- (18) Sheldrick, G. M. *SHELXL-2014/7, Program for the Refinement of Crystal Structure*. University of Göttingen, Germany **2014**.

- (19) Feng, X.; Wang, J. G.; Liu, B.; Wang, L. Y.; Zhao, J. S.; Weng, N. S. From 2D double decker architecture to 3D Pcu framework with 1D tube: syntheses, structures, luminescent and magnetic studies. *Cryst. Growth Des.* **2012**, 12, 927–938.
- (20) Saxena, A.; Kumar, A.; Mozumdar, S. Ni-nanoparticles: an efficient green catalyst for chemo-selective. *J. Mol. Catal. A. Chem.* **2007**, 269, 35–40.
- (21) Bai, R. F.; Feng, X.; Sun, Y. L.; Chen, H.; Qin, G. Z.; Liu, X. F. A silver-organic frameworks based on flexible-aromatic dicarboxylate and bipyridinyl skeletons coligand: crystal structure and luminescence property. *J. Inorg. Organomet. Polym.* **2016**, 26, 512–518.
- (22) Tao, J.; Yin, X.; Wei, Z. B.; Huang, R. B.; Zheng, L. S. Hydrothermal syntheses, crystal structures and photoluminescent properties of three metal-cluster based coordination polymers containing mixed organic ligands. *Eur. J. Inorg. Chem.* **2004**, 1, 125–133.
- (23) Vologzhanina, A. V.; Zorina-Tikhonova, E. N.; Chistyakov, A. S.; Sidorov, A. A.; Russ, A. A. Intermolecular Interactions in crystals of the photosensitive coordination compounds of zinc(II). *J. Coord. Chem.* **2018**, 44, 733–737.
- (24) Wang, Y. F.; He, C. J. Syntheses, crystal structures and characterization of two coordination polymers based on mixed ligands. *Chin. J. Struct. Chem.* **2018**, 37, 481–489.
- (25) Miao, X. H.; Zhu, L. G. Supramolecular assembly under the control of the chelating ligand for the MnII/bridging ligands/3-sulfobenzoate system and catalytic properties for the disproportionation of hydrogen peroxide. *New J. Chem.* **2010**, 34, 2403–2414.
- (26) Feng, X.; Chen, J. L.; Bai, R. F.; Wei, J. T.; Chen, X. X. Two unique cobalt-organic frameworks based on substituted imidazole-dicarboxylate and dipyrindyl-type ancillary ligands: crystal structures and magnetic properties. *Inorg. Chem. Commun.* **2016**, 66, 41–46.
- (27) Stoicescu, L.; Jeanson, A. C.; Tesouro-Vallina, D. A.; Boudalis, A. K.; Costes, J. P.; Tuchagues, J. P. Structure and properties of dinuclear manganese(III) complexes with pentaanionic pentadentate ligands including alkoxo, amido, and phenoxo donors. *Inorg. Chem.* **2007**, 46, 6902–6910.
- (28) Miguel, C. L.; Eugenio, C.; Maurici, L. J. 2D and 3D bimetallic oxalate-based ferromagnets prepared by insertion of Mn III-salen type complexes. *Dalton Trans.* **2013**, 42, 5100–5110.
- (29) Hiller, W.; Strahle, J.; Dtaz, A.; Hanack, M.; Hatfield, W. E.; Haar, L. W.; Gutlich, P. Synthesis, structure, and magnetic properties of catena-(μ -oxo) (hemiporphyrinato) iron(IV), the first polymeric μ -oxo-bridged complex of iron. *J. Am. Chem. Soc.* **1984**, 106, 329–335.
- (30) Han, M. L.; Li, S. H.; Ma, L. F.; Wang, L. Y. Syntheses, structures and properties of two manganese(II) metal-organic frameworks based on bromoisophthalate and bipyridyl-type co-ligands. *Inorg. Chem.* **2012**, 20, 340–345.
- (31) Ma, L. F.; Han, M. L.; Qin, J. H.; Wang, L. Y.; Du, M. MnII coordination polymers based on bi-, tri-, and tetranuclear and polymeric chain building units: crystal structures and magnetic properties. *Inorg. Chem.* **2012**, 51, 9431–9442.
- (32) Ding, S.; Ji, Y. F.; Kang, M. Y.; Du, C. F.; Liu, Z. L.; Liu, C. M. *In situ* synthesis of manganese(III) complexes under control: crystal structure and magnetic properties. *Inorg. Chem. Commun.* **2012**, 21, 96–99.
- (33) Fuller, A. L.; Watkins, R. W.; Dunbar, K. R.; Prosvirin, A. V.; Arif, A. M.; Berreau, L. M. Manganese(II) chemistry of a new N3 O-donor chelate ligand: synthesis, X-ray structures, and magnetic properties of solvent-and oxalate-bound complexes. *Dalton Trans.* **2005**, 1891–1896.